



## Design of potential reverse transcriptase inhibitor containing Isatin nucleus using molecular modeling studies

Vidya Pawar<sup>a</sup>, Deepak Lokwani<sup>a</sup>, Shashikant Bhandari<sup>a,\*</sup>, Debashis Mitra<sup>b</sup>, Sudeep Sabde<sup>b</sup>, Kailash Bothara<sup>c</sup>, Ashwini Madgulkar<sup>a</sup>

<sup>a</sup> Department of Medicinal Chemistry, AISSMS College of Pharmacy, Near RTO, Kennedy Road, Pune 411 001, India

<sup>b</sup> National Centre for Cell Science, NCCS Complex, P. B. No. 40, Ganeshkhind P. O., Pune 411 007, India

<sup>c</sup> Associate Dean, School of Pharmacy & Technology, NMIMS University, Shirpur, Dist.-Dhule, India

### ARTICLE INFO

#### Article history:

Received 1 November 2009

Revised 12 March 2010

Accepted 13 March 2010

Available online 23 March 2010

#### Keywords:

Reverse transcriptase inhibitor

Isatin

Docking, QSAR

### ABSTRACT

Two Dimensional (2D) and Three Dimensional (3D) Quantitative Structure–Activity Relationship (QSAR) studies were performed for correlating the chemical composition of Isatin analogues and their anti-HIV activity using Multiple Linear Regression (MLR) Analysis and k Nearest Neighbor Molecular Field Analysis (kNN MFA), respectively. New Chemical Entities (NCEs) were designed using results of QSAR studies. Binding affinities of designed NCEs were studied on Reverse Transcriptase enzyme using docking studies and their ADME properties were also predicted. Finally most promising compounds were selected from molecular modeling studies. Five compounds containing Isatin nucleus were synthesized and tested for their anti-HIV activity by performing Reverse Transcriptase Assay. Three compounds showed significant Reverse Transcriptase inhibiting activity compared to standard Navirapine. Structure–Activity Relationships were also discussed bases on obtained molecular modeling and experimental data.

© 2010 Elsevier Ltd. All rights reserved.

### 1. Introduction

The origin of Acquired Immunodeficiency Syndrome (AIDS) and the causative organism Human Immunodeficiency Virus (HIV) has puzzled scientists ever since the illness first came to highlight in the early 1980s. Today AIDS is one of the major serious health problems which is caused by HIV-1 virus and has become a major worldwide epidemic.<sup>1,2</sup> At present, the most commonly used anti-HIV therapy is through the concomitant use of drugs that belongs either to the class of nucleoside/nucleotide reverse transcriptase inhibitors (NRTIs/NTRIs) and non-nucleoside reverse transcriptase inhibitors (NNRTIs), protease or entry inhibitors and HIV integrase inhibitors.

NNRTIs are structurally diverse group of compounds which binds to the viral enzyme Reverse Transcriptase (RT) where it interacts with a specific allosteric non-substrate binding pocket site (Non nucleoside binding pocket-NNBP). NNRTIs non-competitively inhibit RT enzyme, block its mechanism and make it unable to produce a viral DNA.<sup>3</sup> Currently drugs used to treat AIDS under NNRTIs for anti-AIDS therapy are Nevirapine, Delaviridine, Efavirenz, Etravirine and Rilpivirine (Fig. 1).

Isatin (1*H*-indol-2,3-dione) analogues, due to the importance of indole back bone have shown a variety of biological activities such as antibacterial,<sup>4,5</sup> antifungal,<sup>5,6</sup> anti-HIV<sup>7,8</sup> and anticonvulsant activity.<sup>9</sup> Owing to the broad spectrum chemotherapeutic proper-

ties, it appears as an ideal drug for AIDS treatment which suppresses HIV replication by acting as non-nucleoside reverse transcriptase inhibitor.<sup>7,8,10–12</sup> Therefore Isatin analogues act as anti-HIV drugs as well as possess efficacy against opportunistic infections associated with AIDS like tuberculosis, hepatitis and other bacterial disease.

NNRTI's belong to widely diverging classes of compounds, closer inspection show that most have some common features, such as carboamide or thiourea entity (body) surrounded by two hydrophobic, mostly aryl moieties (wings). Thus overall structure may be seen as a butterfly with hydrophilic centre (body site A) and two hydrophobic outskirts (wings site B and C)<sup>10</sup> (Fig. 2a).

Also crystal structure analysis of HIV-RT enzyme showed that most of NNRTIs bound to the enzyme in a 'butterfly like' mode.<sup>13,14</sup> One of the wings of this butterfly is made of  $\pi$  electron rich moiety (phenyl or allyl substituents) that interact through  $\pi$ - $\pi$  interaction with a hydrophobic pockets formed mainly by the side chains of aromatic amino acids (Tyr 181, Tyr188, Phe227, Trp229 and Tyr318). On the other hand the other wing is normally represented by a hetero-aromatic ring bearing on one side a functional group capable of donating and/or accepting hydrogen bonds with main chain of Lys 101 and Lys 103, whereas butterfly body, a hydrophobic portion fulfills a small pocket formed mainly by side chains of Lys 103, Val 106 and Val 179 (Fig. 2b).

Molecular modeling study is an approach that used to narrow down a library containing an extraordinarily high number of random molecules into a smaller list of the potentially effective inhibitors. Thus we have focused our aim on computer-aided design

\* Corresponding author. Tel.: +91 9423574082.

E-mail address: [drugdesign1@gmail.com](mailto:drugdesign1@gmail.com) (S. Bhandari).

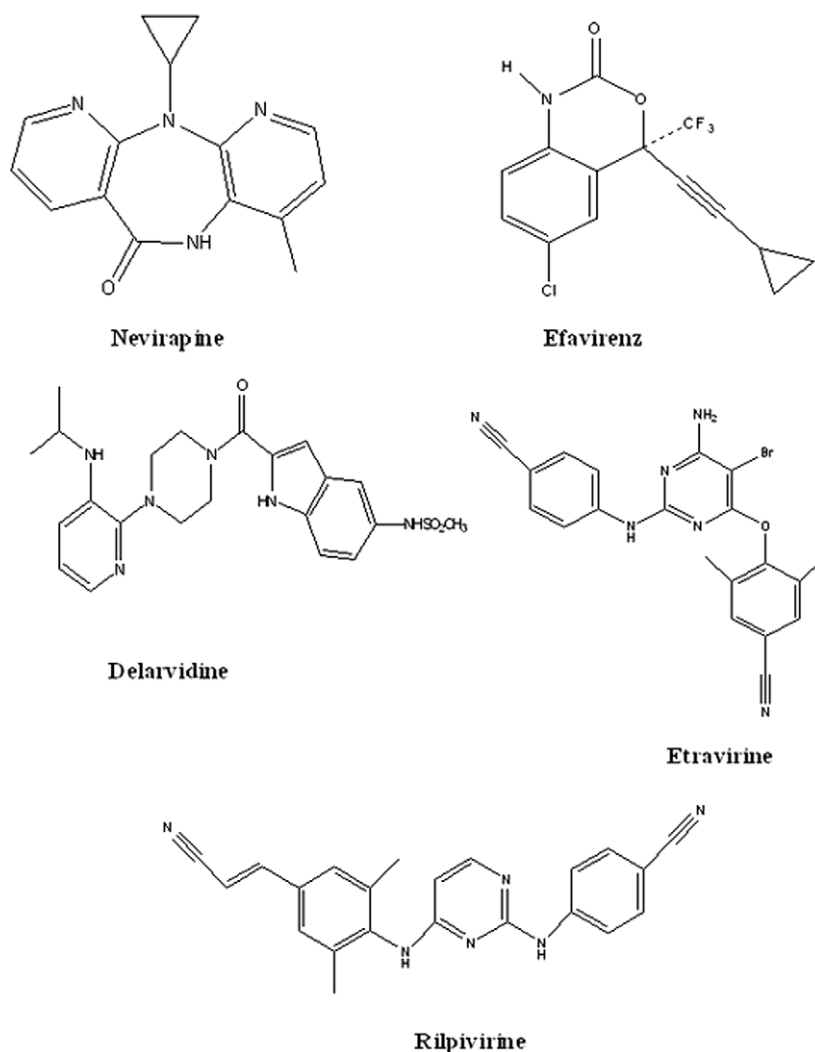


**Figure 1.** Structure of currently used NNRTIs.

of NNRTIs containing Isatin nucleus with simultaneous goals of enhanced performance against RT enzyme. For achieving this aim and optimizing the pharmacophore requirement of Isatin nucleus for design of potent and selective Reverse Transcriptase Inhibitors, we first carried out Two Dimensional (2D) and Three Dimensional (3D) Quantitative Structure–Activity Relationship (QSAR) studies using Multiple Linear Regression (MLR) Analysis and k Nearest Neighbor Molecular Field Analysis (kNN MFA), respectively. New Chemical Entities (NCEs) were designed using information from literature survey and results obtained from 2D QSAR and 3D QSAR studies. In order to gain further insights, we carried out the docking studies on the designed series of NCEs on Reverse Transcriptase (RT) enzyme. ADMET properties were also calculated for ensuring drug like pharmacokinetic profile of the designed NCEs. The most promising compounds were selected on the basis of results of molecular modeling studies and were synthesized and screened for anti-HIV activity by performing the RT assay.

## 2. Results and discussion

### 2.1. QSAR studies

All QSAR studies were performed in V-Life MDS software Version 3.5.<sup>15</sup> A series of 22 compounds of Isatin derivatives tested for their anti-HIV activity was selected for QSAR Studies (Table 1).

Compounds were divided in training and test set. This was achieved by setting aside five compounds as test set which have regularly distributed activity. Selection of molecules in the training set and test is a key and important feature of any QSAR model. Therefore the care was taken in such a way that biological activities of all compounds in test set lie within the maximum and minimum value range of biological activities of training set of compounds. A Uni-Column statistics for training set and test set were generated to check correctness of selection criteria for trainings and test set molecules (Table 2).

The maximum and minimum value in training and set were compared in a way that:

1. The maximum value of  $pEC_{50}$  of test set should be less than or equal to maximum value of  $pEC_{50}$  of training set.
2. The minimum value of  $pEC_{50}$  of test set should be higher than or equal to minimum value of  $pEC_{50}$  of training set.

This observation showed that test set was interpolative and derived within the minimum–maximum range of training set. The mean and standard deviation of  $pEC_{50}$  values of sets of training and test provide insights to relative difference of mean and point density distribution of two sets.

Several 2D QSAR and 3D QSAR models were generated for training set of 17 compounds using MLR and SA kNN MFA (Simulated

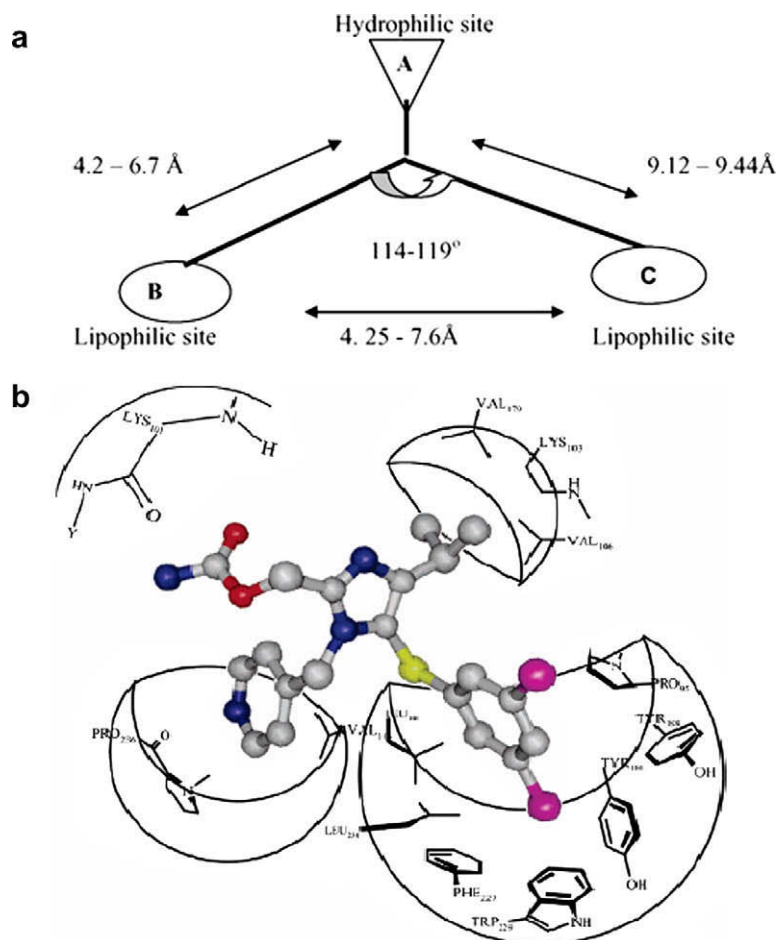


**Figure 2.** (a) Butterfly shape of NNRTIs and distance between hydrophilic centre and two hydrophobic outskirts.<sup>10</sup> (b) Schematic view of the NNBS showing bound conformation of the ligand in the RT complex (PDB Code 1EP4).<sup>14</sup>

Annealing k Nearest Neighbor Molecular Field Analysis) method, respectively. The best QSAR model was selected on the basis of value of Statistical parameters like  $r^2$  (square of correlation coefficient for training set of compounds),  $q^2$  (cross validated  $r^2$ ), and  $\text{pred}_r^2$  (predictive  $r^2$  for the test set of compounds). All QSAR model was validated and tested for its predictability using an external test set of 5 compounds. Statistical results generated by both 2D and 3D QSAR analysis showed that both QSAR model have good internal as well as external predictability (Table 3).

### 2.1.1.1. 2D QSAR

The various 2D QSAR models were developed using MLR method. 2D QSAR equations were selected by optimizing the statistical results generated along with variation of the descriptors in these models. The fitness/pattern plots were also generated for evaluating the dependence of the biological activity on various different types of the descriptors. The frequency of use of a particular descriptor in the population of equations indicated the relevant contributions of the descriptors.

The best regression equation obtained is represented in Eq. 1:

$$\begin{aligned} \text{PEC50} = & -0.0561 \text{ T.O.F.7} + 0.2476 \text{ Polarizability AHC} \\ & + 0.2923 \text{ T.N.N.3} + 0.2298 \text{ H-Acceptor Count} \\ & - 4.8498 \end{aligned} \quad (1)$$

The statistical result of 2D QSAR model along with the contribution of the descriptors is tabulated in Table 3. A brief idea of the requirement of different physicochemical parameters and their contribu-

tions (positive or negative influence on biological activity), required for potential anti-HIV activity was obtained from the 2-D QSAR analysis (Fig. 3).

#### 2.1.1.1. Contribution of descriptors.

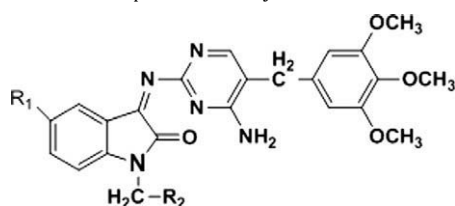
**T\_O\_F\_7:** This is Alignment Independent (AI) descriptors which means the count of number of Oxygen atoms (single double or triple bonded) separated from Fluorine atom by 7 bond distances in a molecule. This descriptor showed negative contribution toward anti-HIV activity in selected QSAR equation (Eq. 1) and its contribution is approx 7% (Fig. 3). Negative contribution of this descriptor revealed the decrease of anti-HIV activity of Isatin analogues with presence of fluorine atom at R<sub>1</sub> position of Isatin ring.

**Polarizability AHC:** This descriptor evaluates molecular polarizability using sum of atomic polarizabilities using the atomic hybrid component (AHC). This is positively contributing descriptor toward anti-HIV activity and its contribution is approx 30%.

**T\_N\_N\_3:** This is also Alignment Independent (AI) descriptors which reveals the count of number of Nitrogen atoms (single double or triple bonded) separated from any other Nitrogen atom (single double or triple bonded) by 3 bonds in a molecule. This is the positively contributing toward anti-HIV activity and it contributes approx 35%. Positive contribution of this descriptor was clearly signifying that presence of Isatin ring containing N–C–C=N group in pharmacophore is important for biological activity.

**H-Acceptor count:** This descriptor signifies Number of hydrogen bond acceptor atoms required in molecule. This is also positively contributing descriptor in selected 2D QSAR equation and its

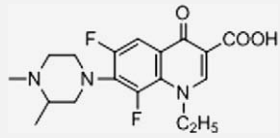
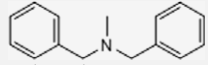
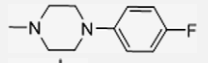
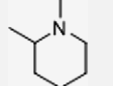
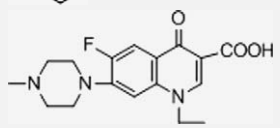
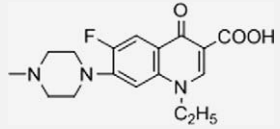
**Table 1**  
Structure of training and test sets of compounds along with observed and predicted activity



Compd	R1	R2	pEC <sub>50</sub>	SA-kNN MFA	
				Predicted activity	Residual
A2	-CH <sub>3</sub>		-1.236	-2.0157	0.0417
A10	-CH <sub>3</sub>		-2.06	-1.8769	0.1849
A11	-CH <sub>3</sub>		-1.453	-1.68729	0.1807
A12 <sup>a</sup>	-CH <sub>3</sub>		-1.326	-1.8269	0.1460
B2	-Br		-1.283	-2.0140	-0.0508
B3	-Br		-0.892	-2.0789	0.0011
B7 <sup>a</sup>	-Br		-1.354	-2.0802	0.05408
B12	-Br		-0.748	-2.0419	-0.0515
B14 <sup>a</sup>	-Br		-1.090	-2.0410	-0.05451
B15	-Br		-0.881	-2.0144	0.0794
F5	-F		-1.559	-2.01072	0.0441
F9 <sup>a</sup>	-F		-1.793	-1.8768	-0.03382
F12	-F		-1.083	-1.8410	0.1966
F13	-F		-1.258	-1.5932	-0.20327

(continued on next page)

Table 1 (continued)

Compd	R1	R2	pEC <sub>50</sub>	SA-kNN MFA	
				Predicted activity	Residual
F14	-F		-1.757	-1.71346	-0.18471
Q1	-Cl		-1.017	-1.81690	0.0295
Q2	-Cl	-N(C <sub>4</sub> H <sub>9</sub> ) <sub>2</sub>	-1.207	-1.78247	-0.16049
Q3	-Cl	-N(C <sub>2</sub> H <sub>5</sub> ) <sub>2</sub>	-1.373	-1.9068	0.2113
Q7	-Cl		-1.749	-1.51321	-0.07659
Q12	-Cl		-1.513	-1.59328	-0.10163
S9	-Br		-1.143	-1.58658	0.0348
S8 <sup>a</sup>	-Cl		-1.053	-1.59328	0.0033

<sup>a</sup> Compounds in test set.

Table 2  
Uni-Column statistics for training set and test set

	Column name	Average (mean)	Max*	Min*	StdDev	Sum
Training set	pEC <sub>50</sub>	-1.3068	-0.7480	-2.0640	0.3489	-22.2160
Test set	pEC <sub>50</sub>	-1.3232	-1.0530	-1.7930	0.2954	-6.6160

Table 3  
Statistical results of 2D QSAR equation generated by MLR method and 3D QSAR model generated by SA kNN MFA method for Isatin derivatives

Sr. No.	Statistical parameter	Results	
		2D QSAR	3D QSAR
1	$r^2$	0.7765	—
2	$r^2SE$	0.2411	—
3	$q^2$	0.6099	0.7322
4	$q^2SE$	0.2174	0.1806
5	Pred_ $r^2$	0.5212	0.7447
6	Pred_ $r^2SE$	0.1646	0.1496
7	F-Test	12.1571	—
8	N	17	17
9	Nearest neighbor	2	2
10	Contributing descriptors	1. Polarizability AHC 2. T_N_N_3 3. H-Acceptor count 4. T_O_F_7	1. S_537 (-0.0109, -0.0066) 2. S_922 (-0.4629, 2.2748) 3. E_144 (0.0675, 0.0008) 4. E_991 (-0.0817, -0.0283)

contribution is approx 28%. This descriptor indicated that presence of hydrogen bond acceptors (C=O group in Isatin ring) in molecule will help to maintain or increase the biological activity of Isatin analogues.

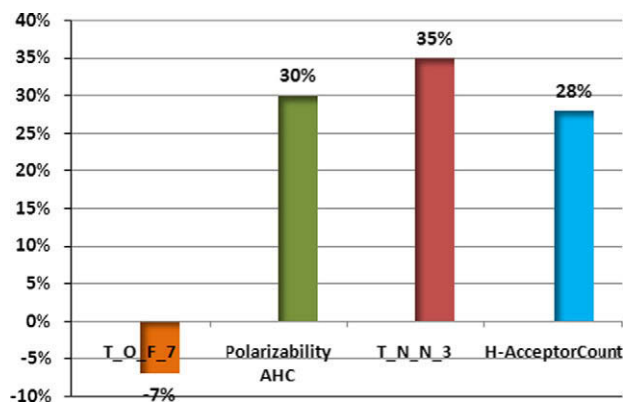


Figure 3. Contributions of descriptors for biological activity developed using MLR equation.

### 2.1.2. 3D QSAR

Several 3D QSAR models were generated using SA kNN MFA method. 3D QSAR models were selected based on value of statistical parameters and the best SA kNN-MFA 3D QSAR model with 17 training compounds have a  $q^2$  ( $r_{cv}^2$ ) of 0.7322 and pred.  $r^2$  of 0.7447 (Table 3).

The kNN MFA QSAR method explores formally the active analogue approach which implies that compounds display similar profiles of pharmacological activities. In this method the activity of each compound is predicted as average activity of k most chemically similar compounds from that data set. The predictive ability of this SA kNN MFA model was evaluated by predicting the biological activities of the test set molecules. Residuals values obtained by subtraction of predicted activities from biological activities were found near to zero. Therefore it was concluded that the resultant QSAR model have good predictive ability. The actual, predicted activities and residuals of both training and test sets molecules are

given in Table 1. The plots of observed versus predicted activity of both training and test sets molecules helped in cross-validation of kNN-QSAR model are depicted in Figure 4.

**2.1.2.1. Interpretation of 3D QSAR studies.** In 3D QSAR studies, 3D data points generated around Isatin pharmacophore were used to optimize the electrostatic and steric requirements of the Isatin nucleus for anti-HIV activity (Fig. 5). The range of property values in the generated data points helped for the design of NCEs. These ranges were based on the variation of the field values at the chosen points using the most active molecule and its nearest neighbor set. The points generated in SA KNN MFA 3D QSAR model are S\_537 (−0.0109, −0.0066), S\_922 (−0.4629, 2.2748) and E\_144 (0.0675, 0.0008), E\_991 (−0.0817, −0.0283) that is, steric and electrostatic interaction field at lattice points 537, 922, 144 and 991, respectively. These points suggested the significance and requirement of electrostatic and steric properties as mentioned in the ranges in parenthesis for structure–activity relationship and maximum biological activity of Isatin analogues.

Negative and positive values in steric field descriptors indicated the requirement of negative and positive steric potential, respectively for enhancing the biological activity of Isatin analogues. Therefore less steric and more steric substituents were preferred at the position of generated data points S\_537 (−0.0109,

−0.0066) and S\_922 (−0.4629, 2.2748), respectively around Isatin pharmacophore. Similarly the positive values of electrostatic descriptors suggested the requirement of electropositive and electronegative groups at the position of generated data point E\_144 (0.0675, 0.0008), and E\_991 (−0.0817, −0.0283), respectively around Isatin pharmacophore for maximum activity. Results obtained and points generated around Isatin pharmacophore using the 3D QSAR studies was used for correlation chemical nature of substituent's around Isatin rings with their observed activity.

**Substitution at R<sub>1</sub>:** 3D QSAR studies helped to find out the importance of electropositive groups at these positions. The electrostatic data point generated was E\_144 (0.0675, 0.0008). It was found that the electropositive groups like methyl, ethyl, propyl, isopropyl, and butyl were essential for potent anti-HIV activity and accordingly the substitutions were carried out for designing of NCEs.

**Substitution at R<sub>2</sub>:** 3D QSAR studies showed requirement of more steric group at R<sub>2</sub> position. The steric data point generated was S\_922 (−0.4629, 2.2748) indicates sterically bulky group like heterocycles, benzene were required at R<sub>2</sub> position.

**Substitution at R<sub>3</sub>:** Two data points generated at the position of R<sub>3</sub> around Isatin nucleus were steric point S\_537 (−0.0109, −0.0066) and electrostatic point E\_991 (−0.0817, −0.0283). These points may show requirement of less steric substituent's containing electronegative groups.

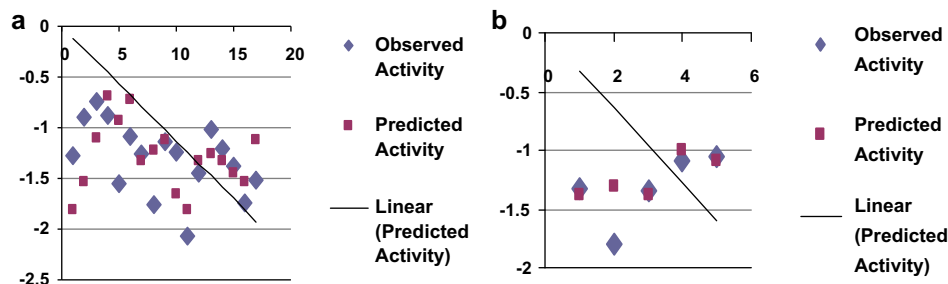


Figure 4. Comparison of observed activity versus predicted activity for (a) training set and (b) test set of compounds.

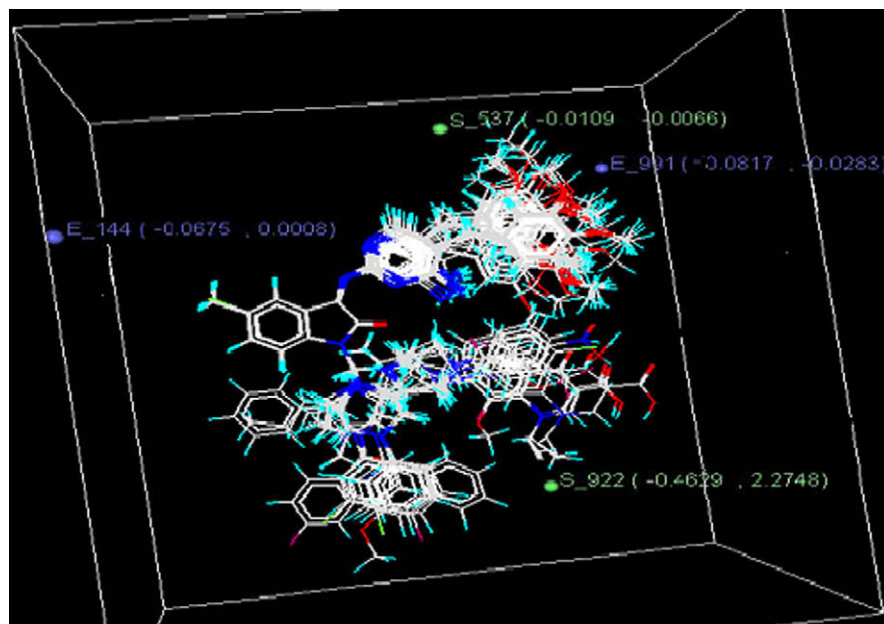


Figure 5. Stereoview of the molecular rectangular field grid around the superposed molecular units of Isatin series of compounds using SA kNN MFA method.

## 2.2. Design of new chemical entities (NCEs) containing Isatin pharmacophore

The findings of 2D and 3D QSAR studies provided the overall substitution pattern (electrostatic, steric and hydrophobic pattern) required around the Isatin pharmacophore (Fig. 6b). Descriptors generated in 2D QSAR equation signified the importance of Isatin nucleus for anti-HIV activity of compounds. Similarly electrostatic and steric points generated around common template or pharmacophore in 3D QSAR suggested substitution of electropositive groups at R<sub>1</sub>, sterically bulky group at R<sub>2</sub> position and less steric substitution at R<sub>3</sub> position around Isatin ring. Hypotheses shown in literature (Section 1) were also consider for optimization of Isatin nucleus in which iminocarbonyl moiety (–N=C–CO–N–) constitutes the body and aryl ring of Isatin bearing one side functional group (donating and/or accepting) and hetero-aromatic ring constitute the wings as shown in (Fig. 6a). This information had helped a lot in optimizing Isatin pharmacophore and designing of NCEs containing Isatin ring for potent anti-HIV activity.

Substitution pattern around Isatin pharmacophore showed in Figure 6 was used for the design of NCEs using CombiLib tool of vLife MDS software. Designed compounds were passed through Lipinski's screen to ensure drug like pharmacokinetic profile of the designed compounds in order to improve their bioavailability. The parameters used as Lipinski's filters are:

1. Number of hydrogen bond acceptor (A) (<10).
2. Number of hydrogen bond donor (B) (<5).

3. Number of rotatable bond (R) (<10).
4. Xlog P (X) (<5).
5. Molecular weight (W) (<500 g/ mol).
6. Polar surface area (S) is (<140 Å).

We had designed 100 compounds containing Isatin nucleus with substitution pattern shown in Figure 6 using CombiLib tool. The columns containing the Lipinski's screen score and other column containing the strings of alphabets, ADRXWS indicating that corresponding compound satisfies all 6 conditions. We have selected 55 compounds based on their predicted activity values and screen scores and results (Table 4). All this compounds were subjected for further studies to sort out the compounds with good binding affinity for RT enzyme and having good ADME properties.

## 2.3. Docking studies

The molecular docking tool, GLIDE<sup>16</sup> (Schrodinger Inc., USA) software was used for studying binding modes of the designed compounds in to the binding pocket of Reverse Transcriptase enzyme. GLIDE was found to produce least number of inaccurate poses and 85% of GLIDES binding models had an RMSD of 1.4 Å or less from native co-crystallized structures.<sup>17</sup> These studies helped to sort out the designed compounds with good binding affinity against RT enzyme. The docking score in terms of G-Score (GLIDE Score), Emodel and other results of docking studies of designed compounds of Isatin series are presented in Table 5.

### 2.3.1. G-score

The scoring function of GLIDE docking program is presented in the G-score form. The G-score indicates the binding affinity of the designed compound to the receptor/enzyme. The G-score of the standard compound Delarvidine was found to be –9.79. The G-score of the designed NCEs N21, N18, N19 and N20 was found to be –11.04, –10.03, –10.24, and –10.09, respectively. The close analysis of these results suggests that the designed NCEs have comparable G-score with the standard compound.

### 2.3.2. H-Bond interactions

H-bond is one of the most widely used parameter for the evaluation of the docking results, as it is an influential parameter in the activity of the drug compound. The number of H-bond interactions in the standard compounds was compared with that of designed NCEs. The number of H-bond in the standard compound Delarvidine was found to be 2 (Fig. 7). The no. of H-bond contact for the designed compounds N21, N18, N19 and N20 were found to be 1, 0, 1, and 1, respectively.

### 2.3.3. Contacts

The contacts are represented in the form of Vender Waals (vdw) Interaction (See supplementary data):

- Good vdw interactions.
- Bad vdw interactions.
- Ugly vdw interactions.

It was found that designed compound N11, N2, N15 and N8 has more number of good vdw interactions, less number of bad vdw and ugly contacts when compared with the standard Delarvidine. But Gscore and Emodel for these molecules were less. In conclusion Gscore and Emodel in addition to number of H-bond interactions, number of good, bad and ugly vdw contact decide the possible binding affinity and in turn potency of the designed NCEs.

N19 showed the H-bond interaction with leucine residue (Fig. 8). The O atom of oxoindole ring of isatin nucleus showed the H-bond interaction with –N–H of leucine (2.357 Å). Methyl

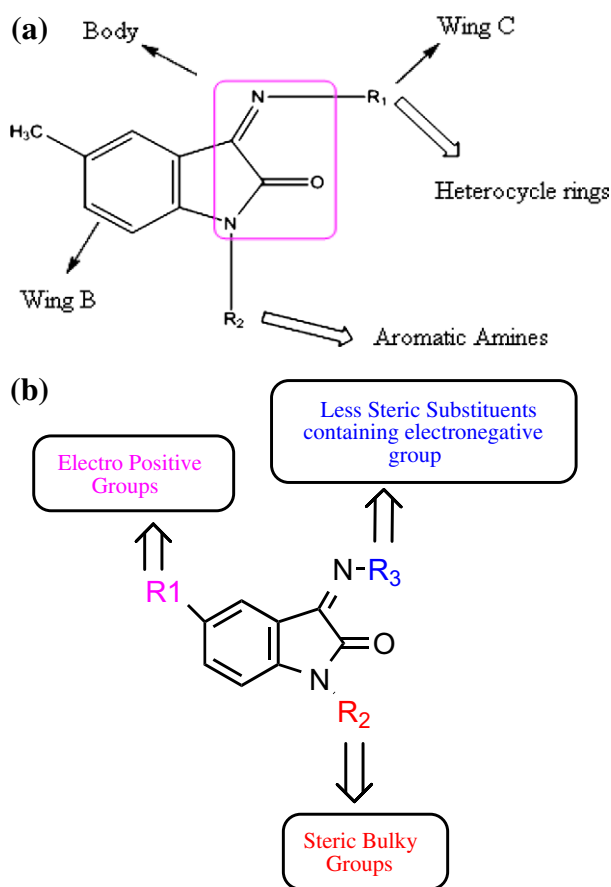
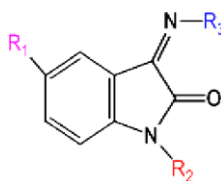


**Figure 6.** (a) Butterfly shape of Isatin along with substituent's to be added. (b) The outcomes of QSAR studies shows requirements around Isatin pharmacophore for anti-HIV activity.

**Table 4**

Structure of designed NCEs along with predicted activity obtained by MLR equation generated by 2D QSAR



Sr. No.	Compd	R1	R2	R3	Screen result	Screen score	Predicted activity
1	N1	-CH <sub>3</sub>	Dimethylamine	Thiazole-1-yl	ADRXWS	6	-3.713
2	N2	-CH <sub>3</sub>	Dimethylamine	Thiazole-1-yl	ADRXWS	6	-2.556
3	N3	-CH <sub>3</sub>	Naphthalene-1-amine	Thiazole-1-yl	ADRXWS	6	-2.391
4	N4	-CH <sub>3</sub>	N-Methyl-1-phenylmethanamine	Thiazole-1-yl	ADRXWS	6	-3.1456
5	N5	-CH <sub>3</sub>	N-Ethylaniline	Thiazole-1-yl	ADRXWS	6	-3.0198
6	N6	-CH <sub>3</sub>	N-Methylaniline	Thiazole-1-yl	ADRXWS	6	-3.0921
7	N7	-CH <sub>3</sub>	Imidazole	Thiazole-1-yl	ADRXWS	6	-2.1992
8	N8	-CH <sub>3</sub>	Morpholine	Thiazole-1-yl	ADRXWS	6	-3.2112
9	N9	-CH <sub>3</sub>	Piperdine	Thiazole-1-yl	ADRXWS	6	-3.9214
10	N10	-CH <sub>3</sub>	Pyrrolidine	Thiazole-1-yl	ADRXWS	6	-2.2256
11	N11	-CH <sub>3</sub>	Piperazine	Thiazole-1-yl	ADWS	4	-3.2318
12	N12	-CH <sub>3</sub>	1-Methyl piperazine	Thiazole-1-yl	ADRXWS	5	-3.2377
13	N13	-CH <sub>3</sub>	1-Methyl piperazine	1,2,4-Triazole	ADRXWS	6	-3.7412
14	N14	-CH <sub>3</sub>	Dimethylamine	1,2,4-Triazole	ADRXWS	6	-1.713
15	N15	-CH <sub>3</sub>	Diethylamine	1,2,4-Triazole	ADRXWS	6	-2.556
16	N16	-CH <sub>3</sub>	Naphthalene-1-amine	1,2,4-Triazole	ADRXWS	6	-3.391
17	N17	-CH <sub>3</sub>	Dibutylamine	1,2,4-Triazole	ADRXWS	6	-3.8456
18	N18	-CH <sub>3</sub>	Morpholine	1,2,4-Triazole	ADRXWS	6	-1.0198
19	N19	-CH <sub>3</sub>	Piperdine	1,2,4-Triazole	ADRXWS	6	-1.0921
20	N20	-CH <sub>3</sub>	Pyrrolidine	1,2,4-Triazole	ADRXWS	6	-2.1992
21	N21	-CH <sub>3</sub>	Piperazine	1,2,4-Triazole	ADRXWS	6	-1.2112
22	N22	-CH <sub>3</sub>	1-Methyl piperazine	1,2,4-Triazole	ADRXWS	6	-1.9214
23	N23	-CH <sub>3</sub>	N-Ethylaniline	1,2,4-Triazole	ADRXWS	6	-2.2256
23	N24	-CH <sub>3</sub>	Dibutylamine	1,2,4-Triazole	ADWS	4	-3.2318
25	N25	-CH <sub>3</sub>	Dibutylamine	Indole	ADRXWS	5	-3.8377
26	N26	-CH <sub>3</sub>	Morpholine	O-Xylene	ADRXWS	6	-3.713
27	N27	-CH <sub>3</sub>	1-Methyl piperazine	O-Xylene	ADRXWS	6	-3.9556
28	N28	-CH <sub>3</sub>	Dimethylamine	Piperazine	ADRXWS	6	-2.391
29	N29	-CH <sub>3</sub>	Piperazine	Piperazine	ADRXWS	6	-3.713
30	N30	-CH <sub>3</sub>	Piperazine	Morpholine	ADRXWS	6	-2.556
31	N31	-CH <sub>3</sub>	Piperdine	Morpholine	ADRXWS	6	-3.991
32	N32	-CH <sub>3</sub>	Pyrrolidine	Morpholine	ADRXWS	6	-2.1456
33	N33	-CH <sub>3</sub>	Diethylamine	Morpholine	ADRXWS	6	-3.0198
34	N34	-CH <sub>3</sub>	Hydrogen	Morpholine	ADRXWS	6	-3.0921
35	N35	-CH <sub>3</sub>	H	Piperazine	ADRXWS	6	-3.1992
36	N36	-CH <sub>3</sub>	H	1,2,4-Triazole	ADRXWS	6	-3.2112
37	N37	-CH <sub>3</sub>	H	Thiazole	ADRXWS	6	-3.2214
38	N38	-Cl	Pyrrrole	Pyridine	ADRXWS	6	-3.9120
39	N39	-Cl	Pyrrrole	Pyridine	ADRXWS	6	-3.6760
40	N40	-Cl	2-Imidazolyl	Imidazole	ADRXWS	6	-3.8889
41	N41	-Cl	Imidazole	2-Imidazolyl	ADRXWS	6	-3.8889
42	N42	-Cl	3-Pyridyl	3-Pyrazolyl	ADRXWS	6	-3.6062
43	N43	-CH <sub>3</sub>	N-Methylaniline	1,2,4-Triazole	ADRXWS	6	-2.2256
44	N44	-Br	2-Pyrrolyl	2-Pyridyl	ADRXWS	6	-3.7524
45	N45	-Br	3-Pyrazolyl	2-Pyrimidinyl	ADRXWS	6	-3.6340
46	N46	-Br	4-Pyrazolyl	3-Pyridyl	ADRXWS	6	-3.5667
47	N47	-Br	Benzopyrrole	Pyridine	ADRXWS	6	-3.6231
48	N48	-Cl	Dibutylamine	Indole	ADRXWS	6	-3.4034
49	N49	-Br	Morpholine	O-Xylene	ADRXWS	6	-3.6340
50	N50	-Br	1-Methyl piperazine	O-Xylene	ADRXWS	6	-3.8965
51	N51	-Cl	Dibutylamine	1,2,4-Triazole	ADRXWS	6	-3.5118
52	N52	-Br	Morpholine	1,2,4-Triazole	ADRXWS	6	-3.4283
53	N53	-Br	Piperdine	1,2,4-Triazole	ADRXWS	6	-3.8293
54	N54	-Br	Dimethylamine	Thiazole-1-yl	ADRXWS	6	-3.6667
55	N55	-Cl	Dimethylamine	Thiazole-1-yl	ADRXWS	6	-3.6340

substitution on 5th position and hetero-aromatic ring substitution act as hydrophobic pocket formed by TYR181, TYR188, PHE-227, and TRP-229. Also other residues lacking H bond may be partially compensated by the involvement of heterocycle moiety  $\pi$ - $\pi$  stacking (TYR181), hydrophobic (TYR188, TRP229) and Vander walls (PRO95, GLU138) interactions. Those residues were found to be in comparable with that standard compound.

#### 2.4. ADMET studies

Prediction of the ADME parameters prior to the experimental studies is one of the most important aspects in the drug discovery and development of the drug molecule. Drug may fail to reach the market phase if those properties are not fulfilled by the drug candidate. Taking into consideration the above mentioned aspects, the

**Table 5**  
Results of Molecular Docking and ADME properties prediction studies

Sr. No.	Compd	G score	Log Po/w	Log S	Log BB	PMDCK	% Absorp.
1	N21	-11.04	2.76	-3.234	0.218	809.105	100
2	Nevirapine	-10.67	3.06	-4.365	0.213	4476.359	100
3	N18	-10.3	3.991	-3.908	-0.185	2646.17	100
4	N19	-10.24	2.081	-2.646	0.118	1336.25	95.63
5	N20	-10.09	0.68	-0.85	-0.192	154.452	75.523
6	Delarvidine	-9.79	2.741	-5.787	-1.672	93.13	84.546
7	N23	-9.51	2.76	-3.234	-0.618	809.105	76
8	N35	-9.37	0.743	-1.82	-0.089	129.45	74.623
9	Efavirenz	-9.34	3.522	-4.834	0.115	6913.027	100
10	N11	-9.28	1.045	-1.312	0.355	475.183	67.646
11	N14	-9.17	3.208	-3.011	0.15	690.8	96.87
12	N7	-9.1	2.081	-2.646	-0.378	1336.25	95.837
13	N34	-9.05	1.286	-2.504	-0.2	1035.51	93.482
14	N2	-9.05	2.175	-1.698	0.194	685.406	91.1
15	N36	-9.03	0.612	-2.164	-0.807	204.325	77.866
16	N15	-8.97	0.872	-0.748	-0.298	160.049	76.906
17	N32	-8.97	1.399	-1.222	0.464	771.495	91.3
18	N8	-8.83	1.162	-0.959	0.268	616.692	84.194
19	N5	-8.81	3.991	-3.908	-0.185	2646.17	60.2
20	N1	-8.73	1.552	-1.334	0.31	688.487	87.272
21	N43	-8.64	2.421	-0.542	0.194	764.155	75
22	N37	-8.48	1.795	-3.012	-0.369	882.611	81.202
23	N16	-8.25	1.999	-2.018	-0.306	176.557	84.21

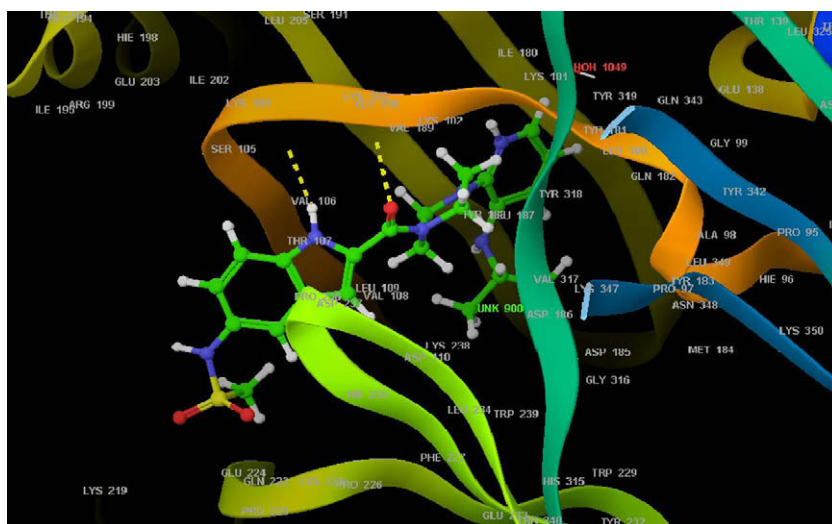


**Figure 7.** Binding mode of standard Delarvidine into binding pocket of RT enzyme.

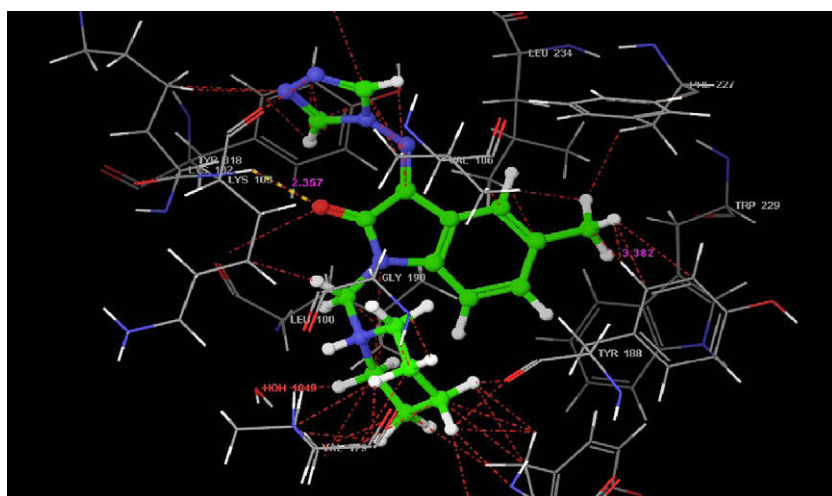


**Figure 8.** Binding mode of standard N19 into binding pocket of RT enzyme.

ADME profile of the designed NCEs was studied using the QikProp<sup>18</sup> tool of Schrodinger software.

In addition to predict molecular properties, QikProp provides the ranges for comparing the molecules properties with those of 95% of known drugs. QikProp also flags 30 types of reactive functional groups that may cause false positives in High Throughput Screen assays (HTS). The range of values that cause a molecule to be flagged can be similar or dissimilar to other known drugs.

Forty four physically descriptors and pharmaceutically relevant properties of Isatin analogues were analyzed using QikProp, among which significant descriptors were reported here required for predicting the drug like properties of molecules (Table 5). These properties were:

1. Molecular weight (mol\_MW) (150–650).
2. Octanol/water partition coefficient (Log Po/w) (–2 to 6.5).
3. Aqueous solubility (QPlog S) (–6.5 to 0.5).
4. Apparent MDCK cell permeability (QPPMDCK) (<25 poor, >500 great).
5. Brain/blood partition coefficient (QP log BB) (–3.0 to 1.2).
6. Percent human oral absorption ( $\geq 80\%$  is high,  $\leq 25\%$  is poor).

The first three properties are based on Lipinski rule of five, molecular weight (mol\_MW) less than 650, partition coefficient between octanol and water (log Po/w) between –2 and 6.5 and solubility (QPlog S) greater than –7. Brain/blood partition coefficient (QPlog BB) parameter indicated about the ability of the drug to pass through the blood–brain barrier which is mandatory for inhibition of some HIV infections. Whereas QPPMDCK Predicted apparent MDCK cell permeability in nm/s. MDCK cells are considered to be a good mimic for the blood–brain barrier, Higher the value of MDCK cell higher the cell permeability. All designed compounds showed ADME properties in acceptable range.

From the results of Molecular modeling studies five compounds (N14, N18, N19, N21 and N43) were selected for synthesis and biological evaluation for anti-HIV activity on RT enzyme.

## 2.5. Chemistry

The synthetic route used to synthesize Isatin analogues is outlined in Scheme 1. In first step, Sandmeyer reaction was carried out which involved the reaction of *p*-toluidine, chloral hydrate and hydroxylamine hydrochloride in aqueous sodium sulfate gave an isonitrosoacetanilide. Later compound after isolation was treated with concd sulfuric acid which gave 5-methyl Isatin. In next step Schiff base were synthesized by condensation of 5-methyl Isatin and 4 amino 1,2,4-triazole in the presence of glacial acetic acid. Finally Mannich reaction of Schiff base gave the target compounds. This reaction involves the condensation of acidic amino group of isatin with formaldehyde and various secondary amines.

All the reactions were monitored by TLC. Structures and purity of the anticipated compounds were characterized by physical constant and FTIR spectral studies followed by <sup>1</sup>H NMR and Mass (GC–MS) analysis. The TLC plates were visualized by Iodine vapors. The reaction products of all the reactions were purified initially by different workup processes to remove unreacted starting materials if any and then by recrystallization using suitable solvents. Most of the steps were optimized in order to achieve quantitative yields that is, more than 70% yields. The physical data, FTIR, <sup>1</sup>H NMR and mass spectral data for all synthesized compounds are reported in experimental protocols.

## 2.6. Biological screening

The anti-HIV activity of synthesized aminopyrimidinimino Isatin derivatives was studied by performing invitro Reverse Transcriptase

Assay. The products were detected and quantified using a colorimetric. Synthesized compound showed comparable inhibitory activity against HIV-1 RT with Nevirapine. Compound N21, N19, N18 emerged as the most potent chemotherapeutic agent's active against HIV. This was revealed that the presence of heterocyclic substituents at R<sub>2</sub> position may increase RT inhibiting activity. However, presence of Aromatic and Aliphatic substitution at R<sub>2</sub> position like in N14 and N43 showed decrease in RT inhabiting activity (Table 6).

## 3. Conclusion

Molecular modeling studies were performed to design NCE's to inhibit RT enzyme for anti-HIV activity. Literature survey and results of QSAR studies revealed that presence of small electropositive group at R<sub>1</sub> position and less bulky group containing electronegative substituent at R<sub>3</sub> position increase the RT inhibiting activity. Also it was proved from designed library of Isatin derivatives that substitution of CH<sub>3</sub> at R<sub>1</sub> position in designed compounds showed better predicted activity than compounds containing –Cl substituent at R<sub>1</sub>.

Thus designed compounds with CH<sub>3</sub> at R<sub>1</sub> position were subjected to docking studies for screening of compounds with good binding affinity for RT enzyme. Docking studies showed that designed compounds and standards bind in same binding pocket containing amino acids Tyr 181, Tyr188, Phe227, Trp229, Tyr318, Lys 101, Lys 103, Val 106 and Val 179 of RT enzyme. Designed compounds containing 1,2,4-triazole at R<sub>3</sub> position showed good binding affinity (G-score) for RT enzyme as compared to compounds with other substituents at R<sub>3</sub> position. Finally most of compounds with CH<sub>3</sub> at R<sub>1</sub> position and 1,2,4-triazole at R<sub>3</sub> were selected for predicting their ADME properties for studying drug like properties.

Five compounds were selected on the basis of results of molecular modeling studies and were synthesized and screened for their anti-HIV activity by performing RT Assay. Compounds N21, N19, N18 showed significant RT inhibiting activity and was found comparable with standard Navirapine. This revealed that the presence of heterocyclic substituents at R<sub>2</sub> position increase RT inhibiting activity of Isatin analogues. However presence of Aromatic and Aliphatic substitution at R<sub>2</sub> position like in N14 and N43 showed decrease in RT inhibiting activity. Thus results of biological evaluation indicated that molecular modeling studies were useful for developing potent compounds for anti-HIV activity.

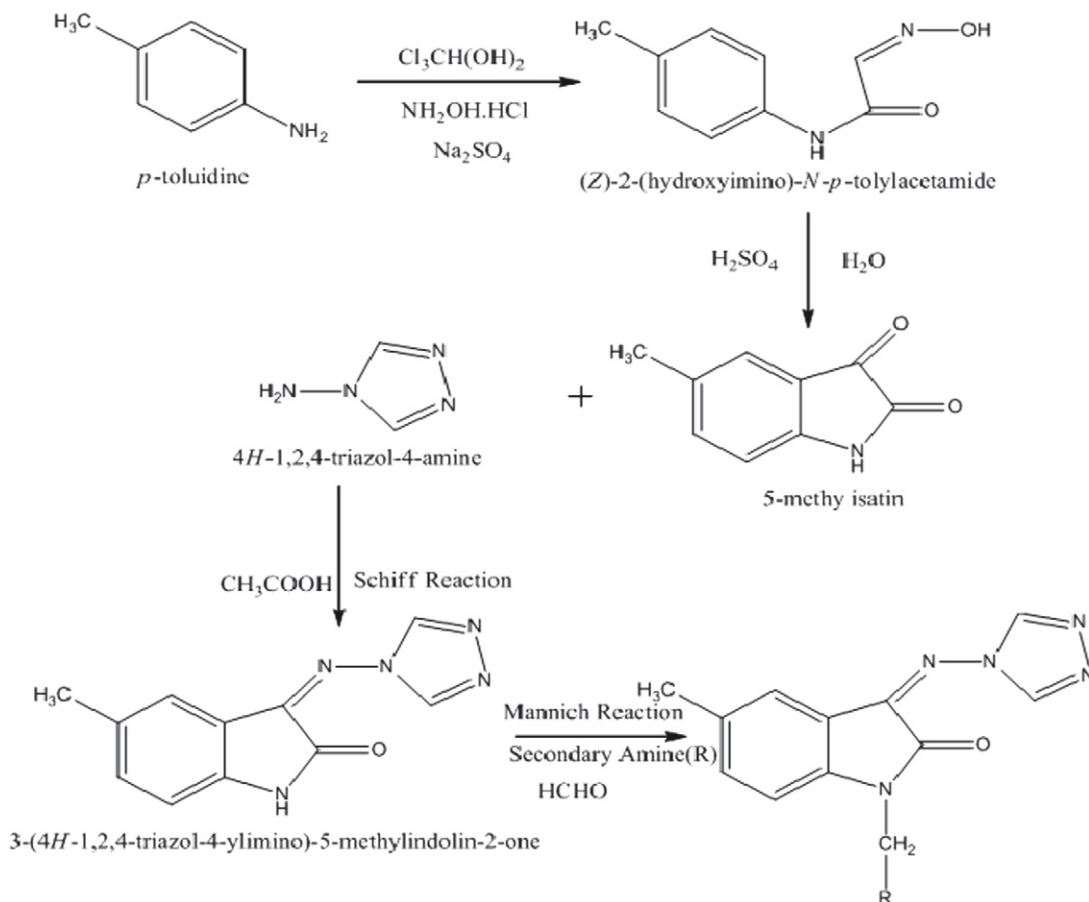
## 4. Experimental

### 4.1. QSAR studies

The structures of all compounds were constructed in the V-life molecular Builder database with standard bond lengths and bond angles. Geometry optimization was carried out using the standard Merck Molecular Force Field (MMFF) with distance dependent-dielectric function and energy gradient of 0.001 kcal/mol Å. The initial conformations were selected and minimized using the Powell method till root-mean-square deviation 0.001 kcal/mol Å was achieved.

#### 4.1.1. Biological data

A data set of 22 compounds of reported series for Anti-HIV activity was used for QSAR study.<sup>10,12,19,20</sup> All QSAR studies were performed using a training set of 17 molecules. A test set of 5 molecules with varied chemical and distributed biological activity was used to assess the predictive power of generated QSAR models. The optimal training and test sets were generated using the sphere exclusion algorithm.<sup>21</sup> The selected series of molecules along with their biological activity data are tabulated in Table 1.



Compounds	-R <sub>2</sub>
N14	Dimethylamine
N18	Morpholine
N19	Piperdine
N21	Piperazine
N43	N-methylaniline

Scheme 1. Synthetic route for Isatin derivatives.

Table 6  
Anti-HIV activity of synthesized compounds against RT enzyme

Compound	Optical density	% Inhibition
Control	1.113	0
Nevirapine	0.089	92.00
N21	0.101	90.91
N19	0.122	89.03
N18	0.177	84.1
N14	0.344	69.1
N43	1.167	0

#### 4.1.2. 2D QSAR studies

The MLR analysis was used to correlate biological activities with physicochemical properties and in turn chemical composition of the selected series of compounds. MLR is the standard method for multivariate data analysis. For getting reliable results, parameters were set such that the regression equation should generate

number of independent variables (descriptors) five times less than that of points (molecules).

The regression equation takes the form as mentioned in Eq. 2:

$$Y = b_1 * x_1 + b_2 * x_2 + b_3 * x_3 + c, \quad (2)$$

where,  $Y$  is the dependent variable (Biological activity,  $\text{pEC}_{50}$ ), the ' $b_1$  to  $b_3$ ' are regression coefficients (contribution of respective descriptors that is,  $x_1$  to  $x_3$ ), ' $x_1$  to  $x_3$ ' are independent variables (Descriptors), and ' $c$ ' is a regression constant or intercept.

#### 4.1.3. 3D QSAR studies

3D QSAR studies were carried out by kNN method using SA as variable selection method. The kNN MFA methodology relies upon a simple distance learning approach. In this method an unknown member is classified according to the majority of its  $k$ -Nearest Neighbors in the training set. The nearness is measured by an appropriate distance metrics (e.g., a molecular similarity measure

calculated using field interactions of molecular structures). The standard kNN MFA method<sup>22</sup> was implemented simply as follows: (i) The distances between an unknown object (*u*) and all other objects in the training set were calculated. (ii) The *k* objects were selected from the training set most similar to object *u*, according to the calculated distances; and (iii) The object *u* was classified with the group to which the majority of the *k* objects belong. An optimal *k* value is selected by optimization through the classification of a test set of samples or by Leave-One Out (LOO) cross-validation. The selected Isatin series of compounds were aligned on the common fragment of oxoindole template using template based alignment method (Fig. 9) and the resulting set of aligned molecules was then used to build 3D QSAR models.

## 4.2. Docking method

The molecular docking tool, GLIDE (Schrodinger Inc., USA) was used for ligand docking studies in to the enzyme Reverse transcriptase binding pocket. The crystal structures of HIV 1 RT were obtained from protein data bank. (PDB Code: 1KLM). All structures were prepared for docking using 'protein preparation wizard' in Maestro wizard 8.5. Water molecules in the crystal structures were deleted and termini were capped by adding ACE and NMA residue. The protein preparation was carried out two steps, preparation and refinement. After ensuring chemical correctness, the hydrogens were added where hydrogen atoms were missing. Side chains that are not close to the binding cavity and do not participate in salt bridges were neutralized. In the refinement component, a restrained impact minimization of the co-crystallized complex was carried out. This helps in reorientation of side chain hydroxyl group. It uses the OPLS-AA force field<sup>23</sup> for this purpose. Grids were defined by centering them on the ligand in the crystal structure using the default box size.

The ligand were built using maestro build panel and prepared by Ligprep 2.2 module which produces the low energy conformer of ligands using MMFF94 force field.<sup>24</sup> The lower energy conformations of the ligands were selected and were docked into the grid generated from protein structures using extra precision (XP) docking mode.<sup>25</sup> In this docking method the ligands are flexible and receptor is rigid except the protein active site which has slight flexibility. The final evaluation is done with glide score (docking score) and single best pose is generated as the output for particular ligand.

$$\text{Gscore} = a \times \text{vdw} + b * \text{coul} + \text{Lipo} + \text{H bond} + \text{Metal} + \text{BuryP} + \text{Rot B} + \text{Site}$$

where, vdW, Van der Waal energy; Coul, Coulomb energy; Lipo, lipophilic contact term; HBond, hydrogen-bonding term; Metal, metal-binding term; BuryP, penalty for buried polar groups; RotB, penalty for freezing rotatable bonds; Site, polar interactions at the active site; and the Coefficients of vdW and Coul are:  $a = 0.065$ ,  $b = 0.130$ .

## 4.3. ADME method

The ADMET properties were calculated using Qikprop tool of Schrodinger software. It predicts both physicochemically significant descriptors and pharmacokinetically relevant properties. It also evaluates the acceptability of analogues based on Lipinski's rule of 5,<sup>26,27</sup> which is essential to ensure drug like pharmacokinetic profile while using rational drug design. All the analogues were neutralized before being used by Qikprop.

## 4.4. Chemistry

All the reactions were carried out with dry, freshly distilled solvents under anhydrous conditions, unless otherwise noted. Melting points were determined by Veego VMP-D Digital melting point apparatus and are uncorrected. FTIR spectra of the powdered compounds were recorded using KBr on a Varian-160 FTIR spectrometer using Diffuse Reflectance Attachment and are reported in  $\text{cm}^{-1}$  and <sup>1</sup>H NMR spectra were recorded on a Varian Mercury YH300 (300 MHz FT NMR) spectrophotometer using TMS as an internal reference (Chemical shift represented in ppm). Purity of the compounds was checked on TLC plates using silica gel G as stationary phase and iodine vapors as visualizing agent.

### 4.4.1. Step I—synthesis of isonitrosoacetop-toluidine<sup>28</sup>

In a 500 ml round-bottomed flask, 9.0 g (0.05 mol) of chloral hydrate and 120 ml of water were placed. To this solution, 130 g of crystallized sodium sulfate; a solution of 5.4 g (0.05 mol) of *p*-toluidine in 30 ml of water and 4.3 ml of concentrated hydrochloric acid (sp. gr. 1.19) and a solution of 11 g (0.15 mol) of hydroxylamine hydrochloride in 50 ml of water were added. The flask was heated over wire gauze and vigorous boiling was begun in about 40–45 min. After 1–2 min of vigorous boiling the reaction was

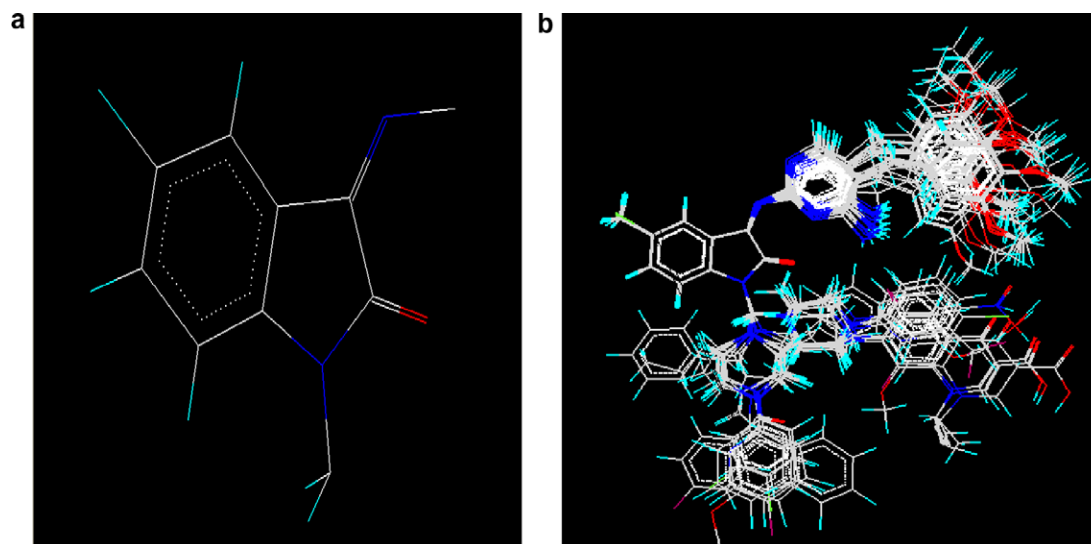


Figure 9. (a) Common template used for alignment of Isatin derivatives and (b) overlay of Isatin series of compounds using V-Life MDS 3.5.

complete. During the heating period, some crystals of isonitrosoacetanilide was separated. On cooling the solution in running water, the remainder crystallized, and was filtered with suction and air-dried. Percent Yield: 84.26% (Solid). Melting point (uncorrected) 160.

#### 4.4.2. Step II—synthesis of 5-methyl Isatin<sup>28</sup>

40.24 ml of concentrated sulfuric acid (sp. gr. 1.84) was warmed to 50 °C in a 250 ml round-bottomed flask fitted with an efficient mechanical stirrer and to this, 10 g (0.05 mol) of dry isonitrosoacetop-toluidine was added at such a rate as to keep the temperature between 60 °C and 70 °C but not higher. External cooling was applied at this stage so that the reaction can be carried out more rapidly. After the addition of the isonitroso compound, the solution was heated to 80 °C and this temperature was kept for about 10 min to complete the reaction. Then the reaction mixture was cooled to room temperature and poured upon 10–12 times its volume of cracked ice. After standing for about one-half hour, the isatin was filtered with suction, washed several times with cold water to remove the sulfuric acid, and then dried in the air. Recrystalline Solvent—Glacial acetic acid, Percent Yield: 86.90% (Solid). Melting point (uncorrected) 178 °C.

#### 4.4.3. Step III—synthesis of Schiff's base<sup>10,12,19</sup>

Equimolar quantities (0.06 mol) of 5-methyl isatin (9.66 g) and 1,2,4-triazole (5.04 g) were dissolved in 75 ml of warm alcohol containing 1 ml of glacial acetic acid. The reaction mixture was refluxed for 4 hours and set aside. The resulting mixture was washed with dilute alcohol, dried. Recrystalline Solvent—ethanol/chloroform mixture, Percent Yield: 77.51% (Solid). Melting point (uncorrected) 199 °C.

#### 4.4.4. Step IV—synthesis of Mannich base (N14, N18, N19, N20 and N43)<sup>10,12,19</sup>

To a slurry consisting (Z)-3-(4H-1,2,4-triazol-4-ylimino)-5-methylindolin-2-one (0.04 mol), 50% ethanol and 37% formalin 1 ml was added to the secondary amine (0.04 mol) dropwise with cooling and shaking. The reaction mixture was allowed to stand at room temperature for 1 h with occasional shaking. The solid product was separated out, filtered and recrystallised.

**4.4.4.1. 3-(4H-1,2,4-Triazol-4-ylimino)-1-((dimethylamino) methyl)-5-methylindolin-2-one (N 14).** Percent Yield: 54.11% (Solid). Melting point (uncorrected) 250 °C. FTIR (KBr):  $\text{cm}^{-1}$  3115 (C–H Stretch); 1697 (C=O Stretch); 1492 (C=N Stretch); 1317 (Ar C–N Stretch); 1178 (Aliphatic C–N Stretch) <sup>1</sup>H NMR (300 MHz, DMSO,  $\delta$  ppm): 2.26 (s, 6H, –CH<sub>3</sub>); 2.34 (s, 3H, –CH<sub>3</sub>); 4.03 (s, 2H, –CH<sub>2</sub>); 7.16–8.02 (m, 3H, Ph); 8.97 (s, 2H, –CH); ESIMS  $m/z$  285.5 [M+1]; Anal. Calcd for C<sub>14</sub>H<sub>16</sub>N<sub>6</sub>O: C, 59.14; H, 5.67; N, 29.56. Found: C, 59.16; H, 5.68; N, 29.57.

**4.4.4.2. 3-(4H-1,2,4-Triazol-4-ylimino)-5-methyl-1-(morpholinomethyl) indolin-2-one (N 18).** Percent Yield: 66.00% (Solid). Melting point (uncorrected) 240 °C. FTIR (KBr):  $\text{cm}^{-1}$  3042 (Ar C–H Stretch); 2827 (Aliphatic C–H Stretch); 1707 (C=O Stretch); 1506 (C=N Stretch); 1059 (Cyclic C–O–C Stretch) <sup>1</sup>H NMR (300 MHz, DMSO,  $\delta$  ppm): 2.30 (s, 3H, –CH<sub>3</sub>); 2.74–2.87 (t, 4H, –CH<sub>2</sub>); 3.21–3.38 (t, 4H, –CH<sub>2</sub>); 4.16 (s, 2H, –CH<sub>2</sub>); 7.78–8.02 (m, 3H, Ph); 8.76 (s, 2H, –CH); ESIMS  $m/z$  326.15 [M+1]. Anal. Calcd for C<sub>16</sub>H<sub>18</sub>N<sub>6</sub>O<sub>2</sub>: C, 58.88; H, 5.56; N, 25.75. Found: C, 58.87; H, 5.58; N, 25.76.

**4.4.4.3. 3-(4H-1,2,4-Triazol-4-ylimino)-5-methyl-1-((piperidin-1-yl) methyl) indolin-2-one (N 19).** Percent Yield: 66.66% (Solid). Melting point (uncorrected) 252 °C. FTIR (KBr):  $\text{cm}^{-1}$  3105 (Ar C–H Stretch); 1683 (C=O Stretch); 1441 (C=N Stretch); 1271 (Ar C–N Stretch); <sup>1</sup>H NMR (300 MHz, DMSO,  $\delta$  ppm) 1.86–2.17 (m, 10H,

–CH<sub>2</sub>); 2.40 (s, 3H, –CH<sub>3</sub>); 4.19 (s, 2H, –CH<sub>2</sub>); 7.38–7.62 (m, 3H, –Ph); 8.87 (s, 2H, –CH); ESIMS  $m/z$  324.14 [M+1]. Anal. Calcd for C<sub>17</sub>H<sub>20</sub>N<sub>6</sub>O: C, 62.95; H, 6.21; N, 25.91. Found: C, 62.96; H, 6.23; N, 25.92.

**4.4.4.4. 3-(4H-1,2,4-Triazol-4-ylimino)-5-methyl-1-((piperazin-1-yl) methyl) indolin-2-one (N 21).** Percent Yield: 66.22% (Solid). Melting point (uncorrected) 269 °C. FTIR (KBr):  $\text{cm}^{-1}$  3438 (N–H Stretch); 3058 (Ar C–H Stretch); 1698 (C=O Stretch); 1488 (C=N Stretch); 1269 (Cyclic C–N Stretch); <sup>1</sup>H NMR (300 MHz, DMSO,  $\delta$  ppm) 1.62 (s, 1H, –NH); 2.18–2.28 (t, 4H, –CH<sub>2</sub>); 2.391–2.48 (t, 4H, –CH<sub>2</sub>); 2.80 (s, 3H, –CH<sub>3</sub>); 3.82 (s, 2H, –CH<sub>2</sub>); 7.57–7.78 (m, 3H, –Ph); 8.59 (s, 2H, –CH); ESIMS  $m/z$  325.25 [M+1]. Anal. Calcd for C<sub>16</sub>H<sub>19</sub>N<sub>7</sub>O: C, 59.06; H, 5.89; N, 30.13. Found: C, 59.09; H, 5.90; N, 30.14.

**4.4.4.5. (Z)-3-(4H-1,2,4-Triazol-4-ylimino)-5-methyl-1-(methyl-(phenyl)amino)methyl)indolin-2-one (N 43).** Percent Yield: 60.16% (Solid). Melting point (uncorrected) 270 °C. FTIR (KBr):  $\text{cm}^{-1}$  3118 (Ar C–H Stretch); 1724 (C=O Stretch); 1520 (C=N Stretch); 1312 (Ar C–N Stretch); 1182 (Aliphatic C–N Stretch) <sup>1</sup>H NMR (300 MHz, DMSO,  $\delta$  ppm): 2.34 (s, 3H, –CH<sub>3</sub>); 3.06 (s, 3H, –CH<sub>3</sub>); 5.03 (s, 2H, –CH<sub>2</sub>); 6.79–7.26 (m, 5H, Ph); 7.16–8.21 (m, 3H, Ph); 8.97 (s, 2H, –CH); ESIMS  $m/z$  346.39 [M+1]. Anal. Calcd for C<sub>19</sub>H<sub>18</sub>N<sub>6</sub>O: C, 65.88; H, 5.24; N, 24.26. Found: C, 65.89; H, 5.24; N, 24.28.

## 4.5. RT inhibiting assay

In a separate reaction tube, 4–6 ng recombinant HIV-1-RT diluted in lysis buffer (20  $\mu$ l/well) was added. Lysis buffer with no HIV-1-RT added was used as a negative control. 20  $\mu$ l of RT inhibitors were diluted in lysis buffer and 20  $\mu$ l reaction mixture (solution 3a or 3b) per reaction tube and incubated for 1 h at 37 °C. For the number of micro plate (MP) modules to be used, enough foil bags were opened and MP modules were put into the frame in the correct orientation. MP modules were ready to use and need not be rehydrated prior to addition of the samples.

The samples (60  $\mu$ l) were transferred into the wells of the MP modules. MP modules were covered with a cover foil and incubated for 1 h at 37 °C. The solution was removed completely and rinsed five times with 250  $\mu$ l of washing buffer per well (solution 6) for 30 s each and washing buffer was removed carefully. 200  $\mu$ l of anti-DIG-POD working dilution (200 mU/ml, solution 5a) were added per well, MP modules were covered with a cover foil and incubated for 1 h at 37 °C. The solution was completely removed. MP modules were rinse five times with 250  $\mu$ l of washing buffer per well (solution 6) for 30 s each and washing buffer was carefully removed. 200  $\mu$ l of ABTS substrate solution (solution 7) was added per well and incubated at +15 to +25 °C until color development (green color) was sufficient for photometric detection (10–30 min). Using microplate (ELISA) reader, absorbance of the samples at 405 nm was measured (reference wavelength: approx. 490 nm).

## Supplementary data

Supplementary data associated with this article can be found, in the online version, at doi:10.1016/j.bmc.2010.03.030.

## References and notes

- Gottlieb, M. S.; Schro, R.; Schankar, H. M.; Weisman, J. D.; Fan, P. T.; Wolf, R. A.; Saxon, A. N. *Eng. J. Med.* **1981**, 305, 1425.
- Barre Sinoussi, F.; Chermann, J. C.; Rey, F.; Nugeyre, M. T.; Chamart, S. *Science* **1983**, 220, 868.
- Balzarini, J. *Curr. Top. Med. Chem.* **2004**, 4, 921.

4. Daisley, R. W.; Shah, V. K. *J. Pharm. Sci.* **1984**, *73*, 407.
5. Varma, R. S.; Nobles, W. L. *J. Med. Chem.* **1967**, *10*, 972.
6. Piscapo, B.; Dium, M. V.; Godliardi, R.; Cucciniello, M.; Veneruso, G. *Bol. Soc. Ital. Biol. Sper.* **1987**, *63*, 827.
7. Pandeya, S. N.; Sriram, D.; Nath, G.; DeClercq, E. *Eur. J. Pharm. Sci.* **1999**, *9*, 25.
8. Pandeya, S. N.; Sriram, D.; Nath, G.; Clercq, D. *Arzneim.-Forsch.* **2000**, *50*, 55.
9. Bhattacharya, S. K.; Chakraborti, A. *Indian J. Exp. Biol.* **1998**, *36*, 118.
10. Sriram, D.; Bal, T. R.; Yogeeswari, P. *IL Farmaco* **2005**, *60*, 377.
11. Boechat, N.; Kover, W. B.; Bastos, M. M.; Romeiro, N. C.; Silva, A. S. C.; Santos, F. C.; Valverde, A. L.; Azevedo, M. L. G.; Wollinger, W.; Souza, T. M. L.; Souza, S.; de Frugulhetti, P. P. *Med. Chem. Res.* **2007**, *15*, 492.
12. Sriram, D.; Bal, T. R.; Yogeeswari, P. *J. Pharm. Pharm. Sci.* **2005**, *8*, 565.
13. Schiifer, W.; Friebe, W.; Leinert, H.; Mertens, A.; Poll, T.; Saal, W.; Zilch, H.; Nuber, B.; Zieglertsf, M. L. *J. Med. Chem.* **1993**, *36*, 726.
14. Ragno, R.; Frasca, S.; Manetti, F.; Brizzi, A.; Massa, S. *J. Med. Chem.* **2005**, *48*, 200.
15. VLife MDS 3.5, Molecular Design Suite, Vlife Sciences Technologies Pvt. Ltd., Pune, India, 2004. ([www.vlifesciences.com](http://www.vlifesciences.com)).
16. GLIDE, Molecular Docking Tool of Schrodinger Inc., version 5.0, New York, USA.
17. Mecllellan, L. M.; Sokol, L. M.; Kontoyiamn, M. *J. Med. Chem.* **2004**, *47*, 558.
18. QikProp, Version 3.0, Schrodinger, LLC, New York, NY, 2005.
19. Sriram, D.; Bal, T.; Yogeeswari, P. *Bioorg. Med. Chem.* **2004**, *12*, 5865.
20. Pandeya, S. N.; Dhamrajan, S.; Nath, G.; Claercq, E. *Eur. J. Med. Chem.* **2000**, *35*, 249.
21. Hudson, B. D.; Rahr, R. M.; Wood, J.; Osman, J. *Quant. Struct.-Act. Relat.* **1996**, *15*, 285.
22. Sharaf, M. A.; Illman, D. L.; Kowalski, B. R. *Chemometrics*; Wiley: New York, 1986.
23. Jorgensen, L.; Maxwell, D.; Tirado-Rives, J. *J. Am. Chem. Soc.* **1996**, *118*, 11225.
24. Hayes, M. J.; Stein, M.; Weiser, J. *J. Phys. Chem.* **2004**, *108*, 3572.
25. Friesner, R. A.; Murphy, R. B.; Repasky, M. P.; Frye, L. L.; Greenwood, J. R.; Halgren, T. A.; Sanschagrin, P. C.; Mainz, D. T. *J. Med. Chem.* **2006**, *49*, 6177.
26. Lipinski, C. A.; Lombardo, F.; Dominy, B. W.; Feeney, P. J. *Adv. Drug Delivery Rev.* **1997**, *23*, 3.
27. Lipinski, C. A.; Lombardo, F.; Dominy, B. W.; Feeney, P. J. *Adv. Drug Delivery Rev.* **2001**, *46*, 3.
28. Gilman, H.; Jeremiah, P.; Gilman, H.. In *Organic Syntheses*; Wayland, E., Ed.; Wiley & Sons: Noland, 1941; Coll. Vol. 1, p 327.